

Cell Reports, Volume 29

Supplemental Information

**B1 and Marginal Zone B Cells but Not
Follicular B2 Cells Require Gpx4
to Prevent Lipid Peroxidation and Ferroptosis**

Jonathan Muri, Helen Thut, Georg W. Bornkamm, and Manfred Kopf

Figure S1

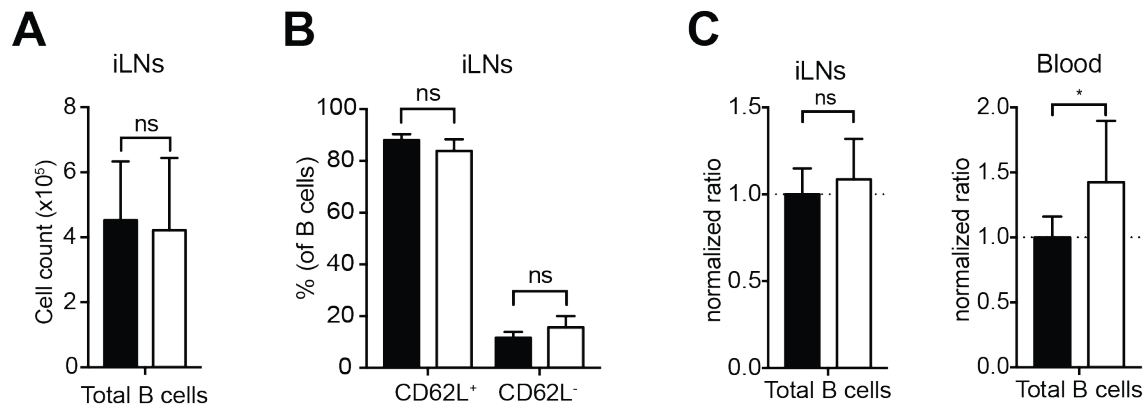


Figure S1. *Gpx4* is dispensable for B-cell homeostasis. Related to Figure 1. (A, B) Analysis of the different B-cell populations in naïve *Gpx4^{fl/fl};Cd19-Cre* and *Gpx4^{fl/fl}* littermate control mice (n = 6). **(A)** Total cell counts of CD19⁺ B cells in the inguinal lymph nodes (iLNs). **(B)** Expression of CD62L on CD19⁺ B cells from the iLNs. **(C)** Lethally irradiated WT mice were reconstituted with a 1:1 mixture of WT and *Gpx4^{fl/fl};Cd19-Cre* bone marrow cells expressing the congenic markers CD45.1 and CD45.2, respectively. After reconstitution, the contribution of *Gpx4^{fl/fl};Cd19-Cre* to the indicated populations in the iLNs (left) and in the blood (right) was assessed. Values were normalized to non-Cre expressing congenic marker-matched TCRβ⁺ T cells, followed by normalization such that CD45.1⁺ WT cell contribution to the respective population equals 1. Values <1 or >1 indicate reduced or higher contribution of *Gpx4^{fl/fl};Cd19-Cre* cells to the B-cell population relative to WT cells, respectively (n = 10). Bar graphs show mean + standard deviation **(A-C)**. Numbers “n” represent individual mice. Data are representative of two independent experiments. Student’s t test (two- tailed, unpaired) was used for the comparison of two groups **(A-C)**: *, P ≤ 0.05; ns, not significant.

Figure S2

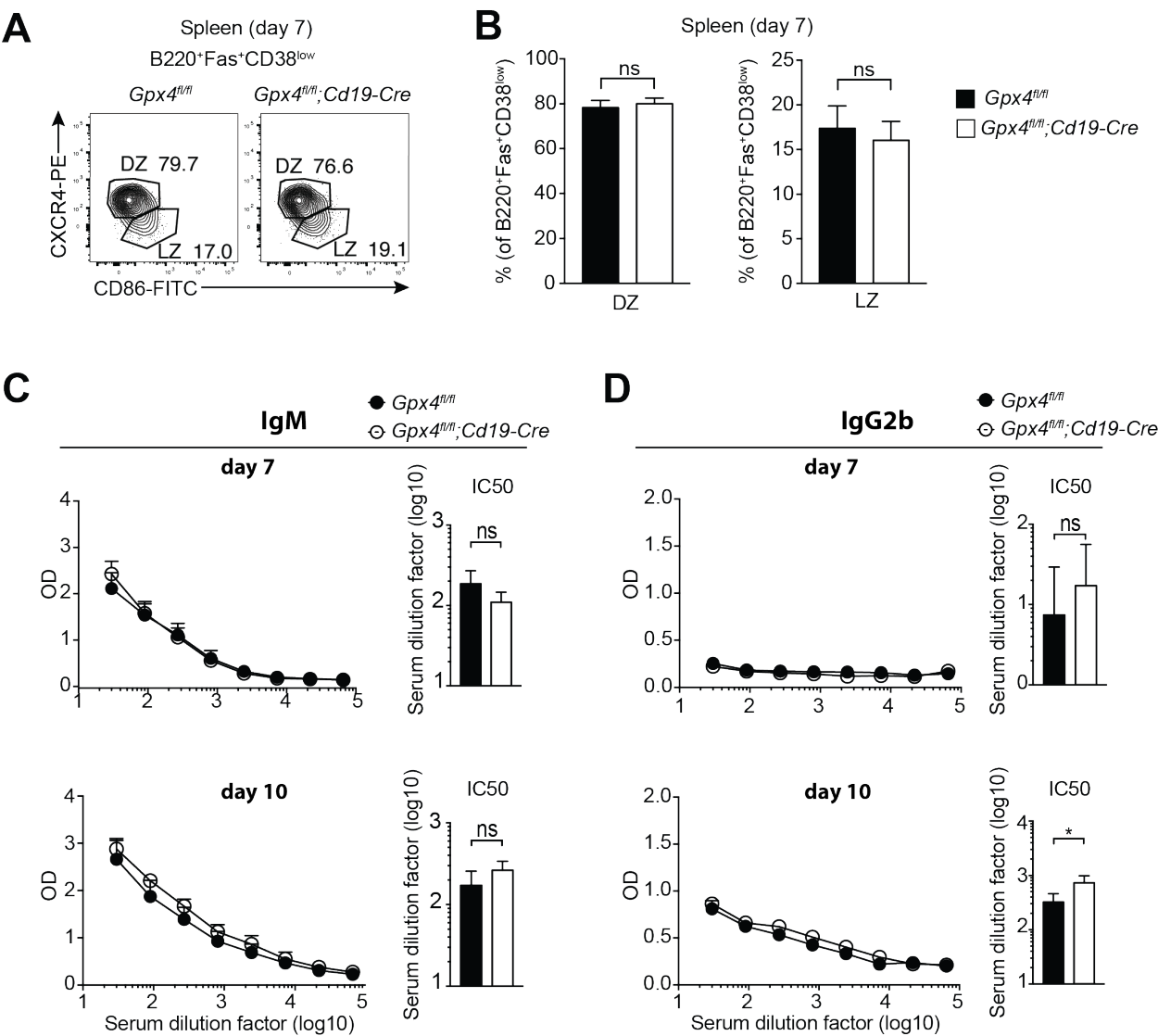


Figure S2. *Gpx4* is not required for B-cell antibody responses and germinal center reactions. Related to Figure 2. (A, B) *Gpx4^{fl/fl};Cd19-Cre* mice and *Gpx4^{fl/fl}* littermate control mice were immunized with Q β -VLPs containing *E. coli* ssRNA. B220⁺Fas⁺CD38^{low} GC B cells were further subdivided into light zone (LZ) and dark zone (DZ) B cells according to expression of CD86 and CXCR4 on day 7 post Q β -VLP immunization. Gating strategy (A) and frequencies (B) of CXCR4⁺CD86⁻ (DZ) and CXCR4⁻CD86⁺ (LZ) B cells are shown (n = 6). (C, D) *Gpx4^{fl/fl};Cd19-Cre* mice and *Gpx4^{fl/fl}* littermate control mice were infected with 100 pfu PR8 influenza A virus. Mice were bled on day 7 (top) and day 10 (bottom) post-infection in order to determine virus-specific IgM (C) and IgG2b (D) antibody responses via ELISA. Each panel depicts plots of OD_{405nm} against serum dilutions (left) and IC₅₀ (right) for virus-specific antibodies (n = 4). Dot plots or bar graphs represent mean + standard deviation (B-D). Numbers “n” represent individual mice. Numbers in the FACS plots indicate the percentage of the depicted gates (A). Data are representative of two independent experiments (A-D). Student's t test (two-tailed, unpaired) was used to compare *Gpx4^{fl/fl};Cd19-Cre* and *Gpx4^{fl/fl}* groups (B-D): *, P \leq 0.05; ns, not significant.

Figure S3

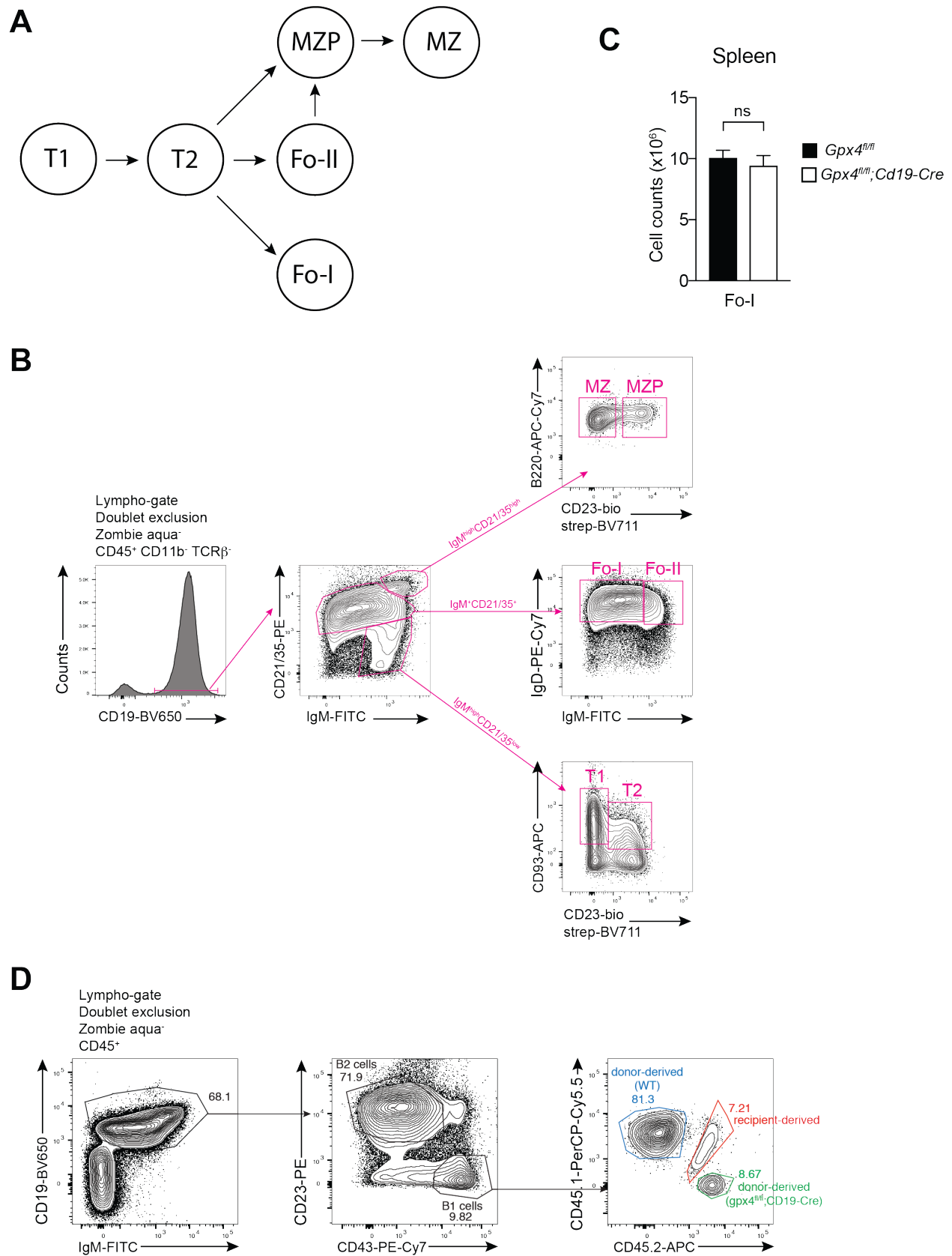


Figure S3. Analysis of the different developing splenic B-cell subsets. Related to Figure 3. (A) Shown is the current model for peripheral B-cell maturation. (B) Gating strategy utilized in this study to identify transitional T1 and T2 cells, follicular (Fo) type I and type II cells, MZ precursors (MZP) and MZ B cells. (C) Total cell counts of Fo type I (Fo-I) in the spleen (n = 6 mice per group). (D) Lethally irradiated WT mice (CD45.1⁺CD45.2⁺) were reconstituted with a 1:1 mixture of WT and *Gpx4^{fl/fl};Cd19-Cre* bone marrow cells expressing the congenic markers CD45.1 and CD45.2, respectively. Shown is the gating strategy utilized to study the potential of Gpx4-sufficient and -deficient bone-marrow to refill the peritoneal B1-cell pool. Bar graphs represent mean + standard deviation (C). Numbers in the FACS plots indicate the percentage of the depicted gates (D). Data are representative of two independent experiments. Student's t test (two-tailed, unpaired) was used to compare *Gpx4^{fl/fl};Cd19-Cre* and *Gpx4^{fl/fl}* groups (C): ns, not significant.

Figure S4

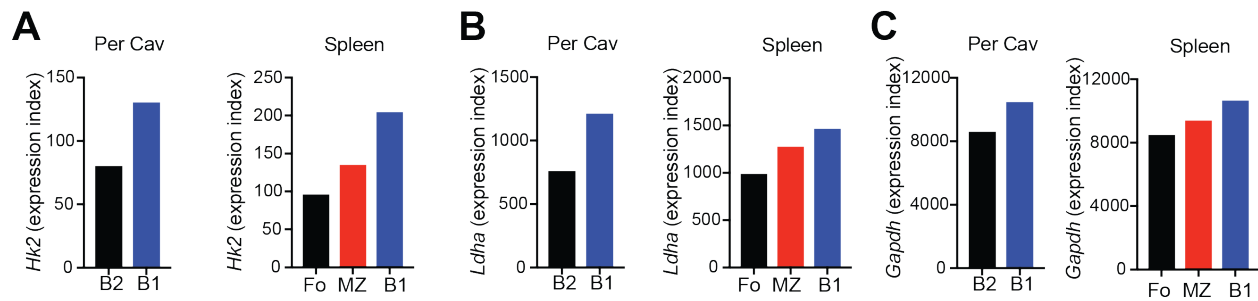


Figure S4. B1 and MZ B cells display increased expression of glycolytic genes. Related to Figure 5. (A-C) Shown are the mean expression values of *Hk2* (A), *Ldha* (B) and *Gapdh* (C) in peritoneal B1 and B2 cells (left) and splenic follicular (Fo), MZ B and B1 cells (right). The expression data were obtained from the Immgen database (mean values).

Figure S5

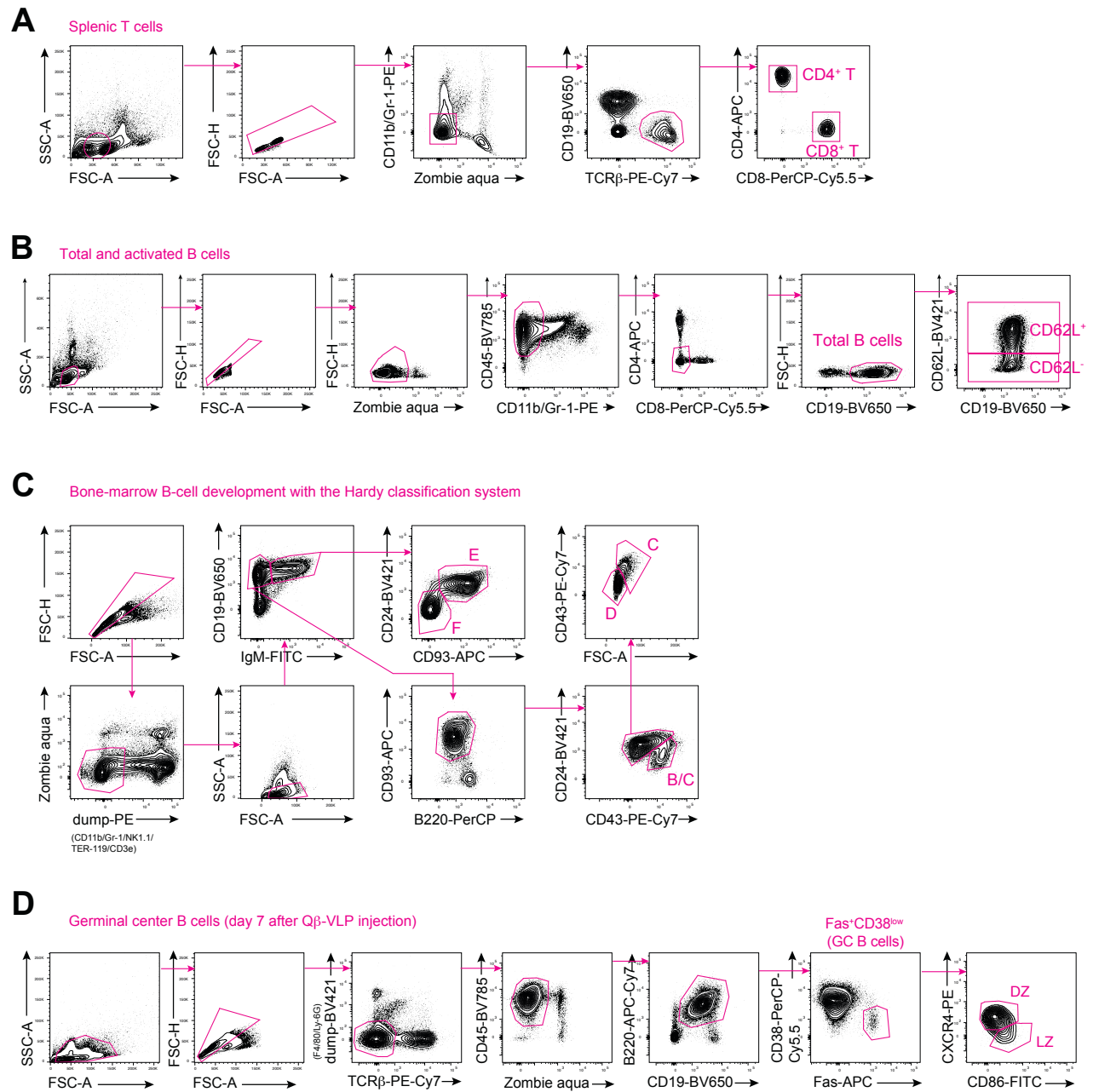
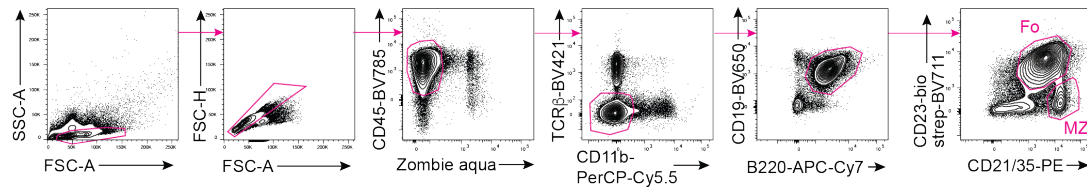


Figure S5. Gating strategies for Figures 1-2. Related to Figures 1-2. (A-C) Representative FACS plots showing gating strategies for Figure 1. **(D)** Representative FACS plots showing the gating strategy for germinal center B cells in Figure 2.

Figure S6

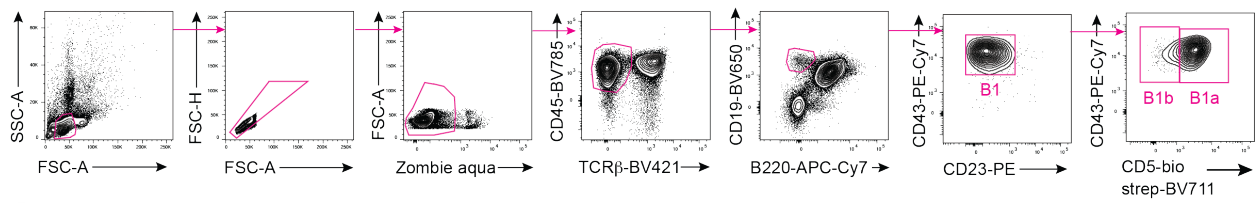
A

Splenic Follicular and MZ B cells



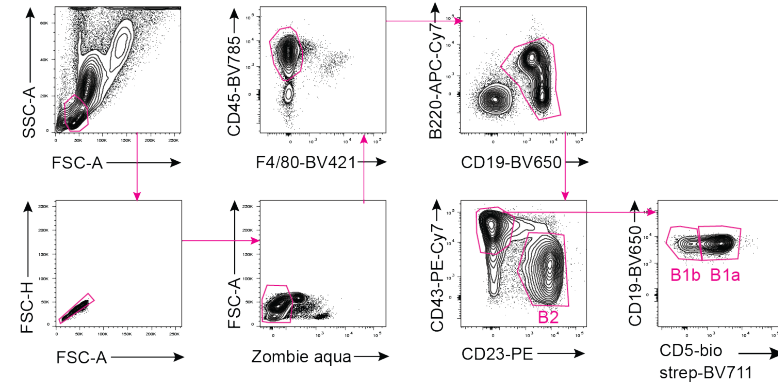
B

Splenic B1 cells



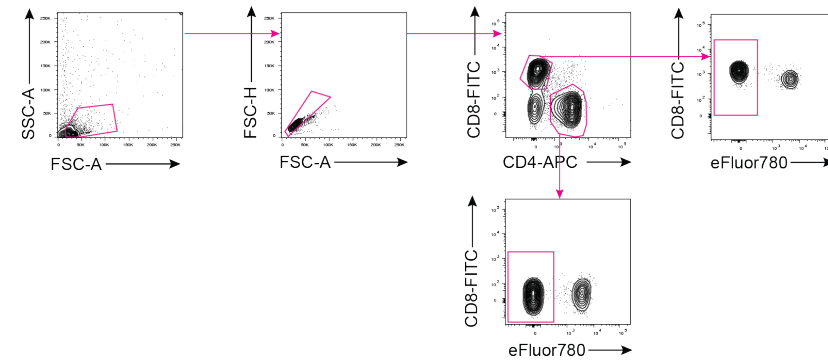
C

B1 and B2 cells in the peritoneal cavity



D

Survival of T cells in vitro



E

Survival of the different B cell populations in vitro

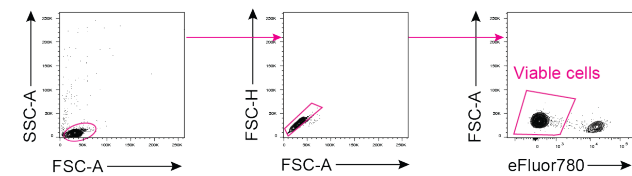


Figure S6. Gating strategies for Figures 3, 5 and 6. Related to Figures 3, 5 and 6.

(A) Representative FACS plots showing gating strategies for follicular B2 and MZ B cells in the spleen (utilized in Figures 3, 5 and 6). (B) Representative FACS plots showing gating strategies for splenic B1 cells (utilized in Figures 3 and 5). (C) Representative FACS plots showing gating strategies for B1 and B2 cells in the peritoneal cavity (utilized in Figures 3, 5 and 6). (D,E) Representative FACS plots showing the gating strategies utilized to study the survival of T cells (D) and of the different B-cell populations (E) in vitro (utilized in Figure 6).